

Simple active stereo vision system for interior room mapping

B. Kaas*¹ and R. Delima ^{a)1}

^{1)McMaster University, 1280 Main Street West, Hamilton, Canada.}

(Dated: 15 December 2017)

This paper demonstrates the operation of a simple, low cost, active stereo vision system for interior room mapping. All the components of the system are consumer grade and accessible to the general public, with an overall cost less than 150 CAD. The system is shown to accurately measure the dimensions of a 239x394 cm room to within 2.1%. Further low cost improvements to the system are discussed.

PACS numbers: 42.30.Wb, 42.30.Tz, 42.79.Qx

Keywords: Active Stereo Vision, 3D mapping, Optical Measurement

I. INTRODUCTION

The level of technological autonomy present today has increased the demand for low cost, non-invasive, optical measurement techniques. Machine vision specifically (stereoscopic or not) plays a large role in process automation. Stereo vision (active or passive) has shown to be a viable approach to 3D profiling¹. It has many practical applications including robot navigation², material deformation measurement³, submarine environment experimentation⁴, and even produce harvesting⁵.

Camera based stereo vision is based off the theory of human stereo vision⁶. The concept uses multiple views of a scene from different projection locations, correlates points in the images, calculates their disparity relative to one another, and uses triangulation to formulate a distance measurement. In theory, distance measurements can be made for each pixel in the overlapping field-of-views of the cameras. This is an advantage stereo vision has over other measurement techniques in that each frame can produce multiple distance measurements.

The two main issues in stereo vision are: the correspondence problem (finding corresponding points of interest between images), and calculating the disparity of corresponding points. Employing an “active” configuration helps to solve the correspondence problem. This is done by projecting structured light patterns onto the object being profiled, thus providing an objective location in each image for correspondence. The disparity of corresponding points must take into account the specific geometry of the device (ie. relative camera locations, variations in camera properties, focal lengths, focal plane array location etc.). This is typically solved through a calibration step where a known distance is measured. A comprehensive mathematical model for obtaining distance measurements and performing the calibration is given by Cardenas-Garcia et al.¹.

The system described here is an active stereo vision system built and tested to 3D profile the interior of a room. Simple consumer webcams and “dollar-store” diode lasers are used for the optical components. The low cost and feasibility of the design acts as a lower bound to the capabilities of such a system. See Table I for the bill of materials.

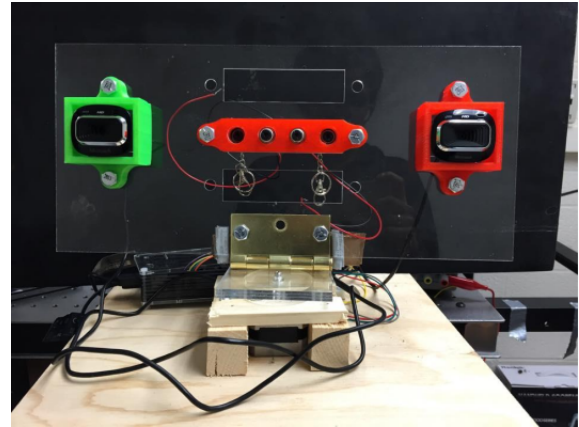


FIG. 1. The experimental setup. Both cameras and lasers are mounted by 3D printed housings which are held together by a piece of acrylic. The stepper motor is encased in wood for stabilization. The raspberry pi, used for image processing, can be seen behind the device.

II. EXPERIMENTAL SETUP

The system consists of two Microsoft LifeCam HD 3000 cameras separated at a distance of 25.9 cm. Three red diode lasers were placed equidistant of each other centered between the cameras. The cameras and lasers were mounted on 3D printed pieces held together by a laser-cut piece of acrylic. The acrylic was mounted with a door hinge to the arm of a stepper motor mounted on a wooden stand ~112 cm high. The device architecture only allows for distance measurements in a single xy plane (where z is vertical). See Figure 1 for a visualization.

The cameras have a horizontal field of view of 59.6 degrees, and the images acquired were 1280x720 pixels in dimension. Each pair of images garnered data for three distance measurements, one from each of the three lasers used during operation. Images were taken every 7.3 ± 0.5 degrees of rotation and processed on the Raspberry Pi via Python OpenCV libraries. The tests were performed with the room lighting off in order to enhance contrast in the images. The processed data was exported to MATLAB where the 2D profile was generated. The whole process took approximately 15 minutes.

TABLE I. Cost breakdown of parts used in the active stereo imaging system.

Component	Cost (\$)
12V Bipolar Stepper Motor	16.48
SN754410 4.5V to 36V Dual Motor Drive	2.76
LifecamHD 3000	30.61 (x2) = 61.22
Lasers	1.70 (x2) = 5.10
Hinge/Bolts/Nails	7.00
Wood	10.00
Acrylic	5.05
Plastic (3D Print)	0.10/g * 3g = 0.30
Total	142.91

Implementation

The distance was extracted from the images using simple triangular geometry and sine law. This is contrary to what was presented by Cardenas-Garcia et al. because it was derived in a more simplistic manner using elementary math.¹ Figure 2 gives the schematic of the model used for calculating the measured distance given by the variable d .

From Figure 2:

$$\frac{l_0}{d} = \tan(\gamma_2) \quad , \quad \frac{l}{d} = \tan(\theta_2)$$

Dividing the previous two equations:

$$\frac{l}{l_0} = \frac{\tan(\theta_2)}{\tan(\gamma_2)}$$

$$\theta_2 = \tan^{-1} \left(\frac{l}{l_0} \tan(\gamma_2) \right) \quad (1)$$

Where l and l_0 are the pixel distances from the centre to the laser spot, and the half the pixel width (640 pixels) respectively; γ_2 is half the horizontal field of view of the camera.

Knowing the angle between the field of view centre and the point of interest for each camera (θ_1 and θ_2), the distance, taken to be the perpendicular distance to the point of interest, is given as follows:

$$\frac{d}{\sin(\alpha)} = \left(\frac{s}{\sin(180 - \alpha - \beta)} \sin(\beta) \right) \frac{1}{\sin(90^\circ)}$$

$$d = s \left(\frac{\sin(\alpha) \sin(\beta)}{\sin(\alpha + \beta)} \right) \quad (2)$$

where α and β are $90 - \theta_2$ and $90 - \theta_1$ respectively. The assumptions made here are three-fold:

1. The distance measured to a point of interest is its perpendicular distance to a point on the line that connects the two cameras, s as per Figure 2.
2. The two cameras' focal plane arrays are in the same plane. Referring to Figure 2, the plane would have unit vectors along the line s and in/out of the page.
3. The field of view for each camera is precise as per the data sheet (no extra measurements were made).

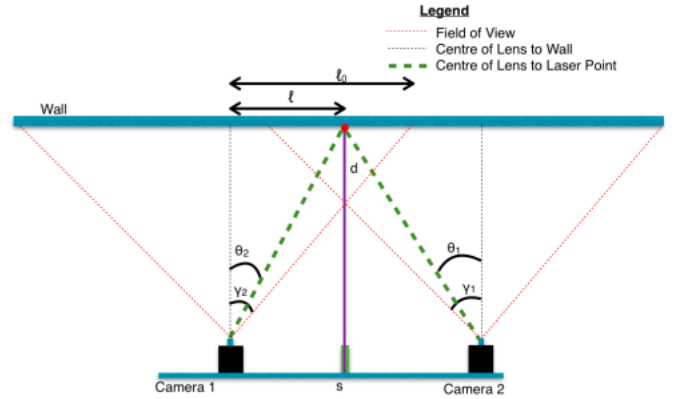


FIG. 2. Model of the experimental setup. The field of view of each camera is drawn as red dotted lines emanating from the black block cameras. These are assumed to begin at the line connecting the two cameras, not offset from the end of the black boxes as shown. Both l and l_0 are distances in image space measured as the number of pixels from the centre pixel to the point of the interest, and half the horizontal number of pixels respectively.

III. RESULTS

Calibration revealed measurement errors of -5% for measurements less than 130 cm, -9% for measurements between 130 cm and 230 cm, and -12% for measurements greater than 230 cm. The negative error measurements imply that the measured distance was systematically less than the actual distances. As per the definition of calibration, the measured systematic error was used to offset the results accordingly. This error is likely due to the assumptions stated in the previous section. Using this template, a room of dimensions 239x394 cm was measured to be 234x391 cm. Thus the overall device error is 2.1% or less. The additional error can be attributed to the piecewise calibration correction function over three intervals as opposed to finding a continuous correction function of distance. A schematic of the final output of the system is shown in Figure 3. Sample points at different azimuthal angles for the system operating with two lasers are given in Table II.

The results given are of a small sample size and only pertain to one room. This may seem to limit the repeatability of the system, however the main focus of this

TABLE II. Example of distance data points at different azimuthal angles collected with only two lasers employed.

Azimuthal Angle	Distance Measurements	
	Left Laser (in)	Right Laser (in)
7°	47.123	47.239
14°	47.175	47.436
21°	47.317	47.382
28°	48.199	49.714
35°	50.904	51.984
42°	53.530	55.534

undertaking was to obtain an affordable and feasible solution for active stereo vision. Many improvements to the device can be made including scan time (capture video to limit stop time), addition of a height dimension through larger area active illumination or more robust correspondence algorithms between images, more precise opto-mechanics to enable finer alignment and remove unwanted vibrations or optical element shifting during operation, and more accurate calibration techniques to name a few. All of these improvements, except more precise opto-mechanics, do not involve a large increase in cost to the device.

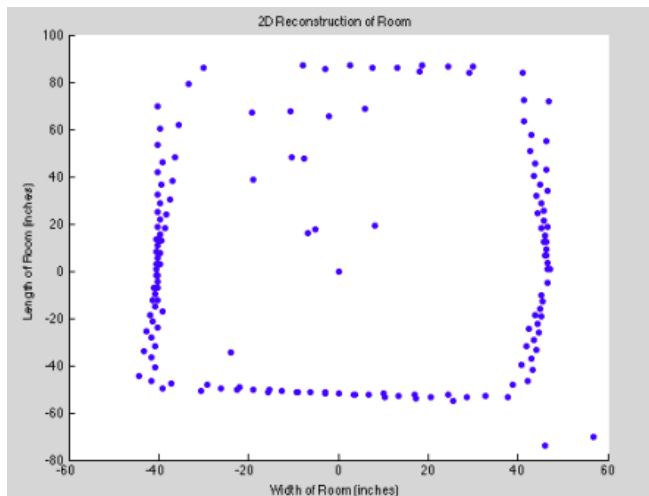


FIG. 3. Reconstructed 2D data point map of the room dimensions. Each axis measured in inches. Each data point on the plot represents a measured distance ie. one of the laser points in an image pair.

IV. CONCLUSIONS

It has been shown that an active stereo vision measurement system costing less than \$150 is capable of measuring the dimensions of a 239x394 cm room to within 2.1%. All the components used to make the device are accessible materials except for the processing of the laser cutter and the 3D printed mounts.

ACKNOWLEDGMENTS

B. Kaas wishes to acknowledge Dr. A. Turak for the opportunity and guidance provided to complete this paper. B. Kaas also wishes to acknowledge Roxanna Delima for her large contributions to the project.

Notes and References

^{a)}B. Kaas and R. Delima contributed equally to this work.

*Author to whom correspondence should be addressed: kaasbw@mcmaster.ca

- ¹J. F. Cardenas-Garcia, H. G. Yao, and S. Zheng. 3d reconstruction of objects using stereo imaging. *Optics and Lasers in Engineering*, 22(3):193–213, January 1995. ISSN 0143-8166.
- ²D.J. Kriegman, E. Triendl, and T.O. Binford. Stereo vision and navigation in buildings for mobile robots. *Robotics and Automation, IEEE Transactions on*, 5(6):792–803, 1989. ISSN 1042-296X.
- ³Per Synnergren and Mikael Sjdahl. A stereoscopic digital speckle photography system for 3-D displacement field measurements. *Optics and Lasers in Engineering*, 31(6):425–443, 1999. ISSN 0143-8166.
- ⁴F. Bruno, G. Bianco, M. Muzzupappa, S. Barone, and A. V. Rationale. Experimentation of structured light and stereo vision for underwater 3d reconstruction. *ISPRS Journal of Photogrammetry and Remote Sensing*, 66(4):508–518, July 2011. ISSN 0924-2716.
- ⁵Feng Qingchun, Cheng Wei, Zhou Jianjun, and Wang Xiu. Design of structured-light vision system for tomato harvesting robot. *International Journal of Agricultural and Biological Engineering*, 7(2):19–26, April 2014. ISSN 1934-6352.
- ⁶D. Marr and T. Poggio. A computational theory of human stereo vision. *Proc. R. Soc. Lond. B*, 204(1156):301–328, May 1979. ISSN 0080-4649, 2053-9193.